Flexible UV sensor based on nanostructured ZnO thin film SAW device

Hasan, Sameer Ahmad; Torun, Hamdi; Gibson, Des; Wu, Qiang; Cooke, Michael D.; Fu, YongQing

Published in:
2019 IEEE Jordan International Joint Conference on Electrical Engineering and Information Technology (JEEIT)

DOI:
10.1109/JEEIT.2019.8717373

Published: 20/05/2019

Document Version
Peer reviewed version

Flexible UV sensor based on nanosturctured ZnO thin film SAW device

Sameer Ahmad Hasan
Facullty of Engineering and Environment
Northumbria University
Newcastle upon Tyne, UK
sameer.hasan@northumbria.ac.uk

Hamdi Torun
Facullty of Engineering and Environment
Northumbria University
Newcastle upon Tyne, UK
Hamdi.torun@northumbria.ac.uk

Des Gibson
Institute of thin films, sensors and imaging
University of West of Scotland
Paisley, PA1 2BE
Des.Gibson@uws.ac.uk

Qiang Wu
Facullty of Engineering and Environment
Northumbria University
Newcastle upon Tyne, UK
qiang.wu@northumbria.ac.uk

Michael D. Cooke
Departemnt of Engineering
Durham University
Durham, DH1 3LE
michael.cooke@durham.ac.uk

YongQing Fu
Facullty of Engineering and Environment
Northumbria University
Newcastle upon Tyne, UK
Richard.fu@northumbria.ac.uk

***Abstract*—An ultraviolet (UV) light sensor was developed using flexible SAW device based on ZnO thin film deposited onto low cost and commercial aluminum foil. ZnO nanorods were further grown on the surface of the SAW device for enhancing the sensitivity. The zero order lamb wave modes were identified and used to obtain their frequency responses at various UV light intensities. UV Sensing performance was investigated in different flexible/bending positions and the results exhibited a very good sensitivity and great potential for flexible and wearable UV light sensing applications.**

Keywords—ZnO thin film, ZnO nanowires, flexible SAW devices, UV sensing

I. INTRODUCTION

Zinc oxide (ZnO) thin film-based surface acoustic wave (SAW) devices have been extensively studied for their potential uses in various sensing applications such as humidity, temperature, environmental, chemical and biological sensing. These devices generally exhibit high efficiency, good performance, high sensitivity and reliability. In addition, they have compact design, can be manufactured at low cost and can be easily integrated with other microsystems and lab-on-a-chip platforms. Moreover, they can be used as remote sensors due to their capability to perform as wireless detectors [1-3].

Ultraviolet (UV) light has been commonly utilised in biomedical applications, astronomy, space communication and water treatment. Therefore, it has attracted great attention in order to monitor and control the level of UV dosage and exposure. Owing to a band gap energy of 3.37 eV at room temperature, a large exciton binding energy of 60 meV and attractive optical and piezo-electrical properties, ZnO thin film has been considered as a suitable material for UV detection [4-6].

The main principle of UV detection using the ZnO thin film based SAW sensors depends on creations of electron-hole pairs in ZnO thin film when it is illuminated with UV light. This causes changes of its surface sheet conductivity and results in the changes in acoustic wave velocity which can be measured as a function of frequency shift [7].

The surface of ZnO thin film has extra free electrons due to the existence of intrinsic defects where oxygen molecules from the surrounding environment are chemically adsorbed onto the surface and capture those electrons [8].

$$O_{2(gas)} + 2\ \text{electrons}^- \rightarrow O_2^{--} \quad (1)$$

When the surface is illuminated with UV light, UV photons interact with ZnO thin film by generating electron-hole pairs since the UV photons have higher bandgap energy than that of ZnO. Thus, the recombination of the confined electrons and holes will release the adsorbed oxygen molecules back to atmosphere and results in increase of the surface sheet conductivity of ZnO thin film [8, 9].

$$2\text{Holes}^+ + O_2^{--}{}_{(\text{adsorbed})} \rightarrow O_{2(gas)} \quad (2)$$

This change will influence the phase velocity of the acoustic wave due to the acoustic-electrical interactions and it can be estimated using the following equation [7, 10]:

$$\frac{\Delta v}{v_0} = -\frac{k^2}{2}\frac{1}{1+\sigma_s^2/\sigma_m^2} \quad (3)$$

$$\Gamma = k^2 \frac{\Pi}{\lambda}\frac{\sigma_s\,\sigma_m}{\sigma_s^2+\sigma_m^2} \quad (4)$$

Where v is the acoustic velocity, k^2 is the electromechanical coupling coefficient, σ_s is the surface sheet conductivity, σ_m is the sheet conductivity of ZnO bulk material, Γ is the insertion loss and λ is the wavelength.

Nanostructured materials such as ZnO nanorods and ZnO nanoparticles have been exploited to enhance the sensitivity of UV light sensing. The large surface-to-volume ratio of the nanostructures increases light absorption and decrease losses that eventually enhances light scattering and improves the sensitivity of the photosensitive film [11-15].

However, most of SAW UV sensors reported in literature are fabricated on rigid substrates such as ZnO/$LiNbO_3$, ZnO/Si and ZnO/36° Y-cut $LiTaO_3$ where the Rayleigh mode is commonly used for UV detection. These devices lack flexibility to be fitted onto non-flat or complex surfaces. However, the demand for flexible and bendable sensors have been remarkably increased driven by the significant needs of wearable technology for continuous real-time monitoring and the development of flexible electronics. Therefore, ZnO thin film has been deposited onto flexible substrates such as Kapton polyimide (PI) to produce Lamb wave sensors for UV and other sensing applications [13, 16-18].

In this paper, a low cost and flexible SAW (Lamb wave) UV sensor has been developed by depositing ZnO thin film onto a commercial aluminium foil. In addition, ZnO nanorods

have been grown on the surface of the device to enhance its sensitivity. The sensor has exhibited excellent performance under various flexible/bending positions with high sensitivity and reliability. It makes this device very promising for flexible and wearable applications.

II. Methodology

Direct current (DC) magnetron sputtering system (Nordiko 3750) with Zn targets (99.99% purity) was used to deposit ZnO thin film on the commercial aluminium foil (50 µm thick). The deposition parameters were listed as follows: DC power 400 W, Ar flow rate 6.5 sccm (standard cubic centimetre per minute) and O_2 flow rate 13.0 sccm. X-ray diffraction (XRD) and scanned electron microscope (SEM) were used to characterise film properties such as film crystallinity, thickness and film microstructures. Periodic Cr/Au (80/120 nm) interdigital transducers (IDTs) were patterned using conventional photolithography and lift-off processes to fabricate SAW devices with a wavelength of 160 µm. Keysight N9913A Fieldfox vector network analyser was used to obtain the frequency response of the device.

ZnO nanorods were grown on the delay line region of the SAW device using a hydrothermal technique as illustrated in figure 1. The process has been done by growing the nanorods on the top of the thin film without depositing an insulating layer or a seed layer. A precursor solution of zinc nitrate ($Zn(NO_3)_2$, $\geqslant$ 99.0% purity) from Sigma-Aldrich was prepared in a sealed container. The PH value was adjusted to 10.3 by adding ammonium hydroxide (NH_4OH, $\geqslant$ 99.99%) obtained from Sigma Aldrich without other materials such as methenamine. The SAW device was suspended (upside down) on the surface of the solution where ZnO thin film was in contact with the solution. The temperature was set at 85°C and the device was kept in the solution for 4 hours, then it was rinsed with deionized water to remove any reaction residues. Crosse section and nanorods morphology were characterised using SEM [13, 19].

A UV light source (CS2010, Thorlabs) with wavelength (λ) of 365 nm was used to illuminate the surface of the device that was placed in a fixed distance of 6.0 cm from the source. The UV intensity was controlled in percentage of the maximum power where a reference photodiode power sensor (S120VC, Thorlabs) was used to measure the corresponding UV intensity. The UV light intensity was varied from 1 to 26 mW/cm^2. A digital temperature sensor (SHT71, Sensirion) was attached to the surface of the SAW device to monitor any temperature variations.

The signals from the network analyser was controlled using a LabView based software programme through a network cable. The frequency response of the reflection (S11) and the transmission (S21) signals of the SAW device were measured when it was illuminated with UV light at different positions: e.g., flat, bending down and bending up (bending radius was 10 mm) as shown in figure 2.

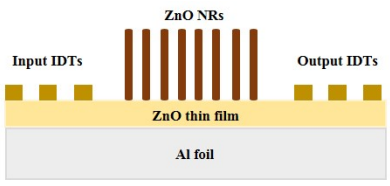

Fig. 1 SAW device structure with ZnO nanorods

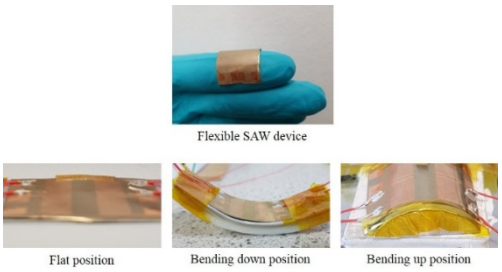

Fig. 2 SAW device in different flexible and bent positions

III. Results and Discussion

Figure 3 shows SEM surface morphology of the deposited ZnO thin film. The results indicate that the thin film has a granular structure composed of large ZnO grains with an estimated average size of 350 nm. The top surface has no cracks or apparent defects. The thickness of the film was measured at different locations over the substrate and it was in the range of 4.0 – 6.5 µm.

The XRD analysis of the ZnO film is shown in figure 4. It reveals a sharp peak at 2θ of 34.5° corresponding to a strong C-axis orientation perpendicular to film plane (002) (card # 79-207). The full width half maximum (FWHM) value is 0.144° indicating a small dispersion of the crystallites and high quality of film crystalline structures. Another weak peak of ZnO (100) at 31.1° can be noticed, in addition to a small peak at 45.0° that is corresponding to aluminium substrate (card # 65-2869).

Figure 5 shows the morphology of ZnO nanorods grown on the top surface of ZnO thin film. They are dense and aligned in a forest shaped columnar orientation perpendicular to the surface. The estimated length and diameters of the nanorods are 0.9 - 1.1 µm and 60 – 160 nm, respectively.

The transmission (S_{21}) and the reflection (S_{11}) spectra of the SAW device are shown in figure 6. It shows that the zero order of the antisymmetric mode (A0) of Lamb wave is present at 13 MHz and the symmetric mode (S0) at 30 MHz and they match the vibrating modes for the same device with a wavelength of 160 µm reported in Ref. [20].

These two modes were used to investigate the performance of this SAW device as a flexible UV sensor.

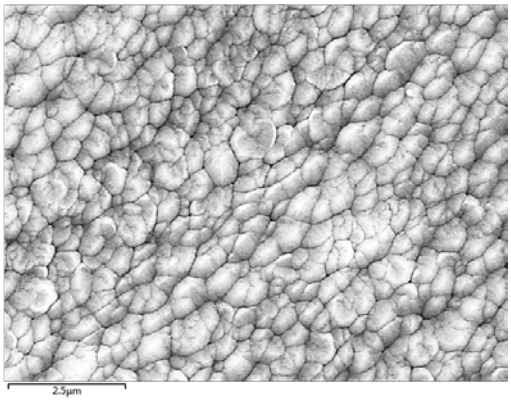

Fig. 3 SEM surface morphology of ZnO thin file on Aluminum foil

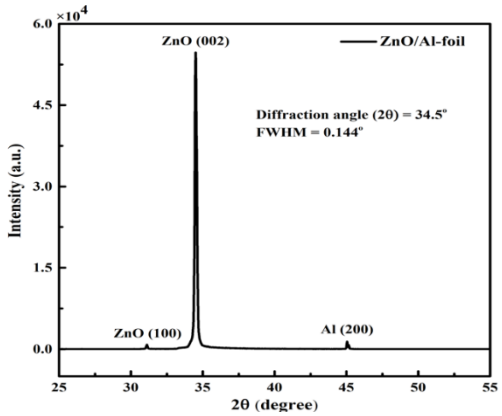

Fig. 4 XRD characterization of ZnO thin film on Aluminum foil

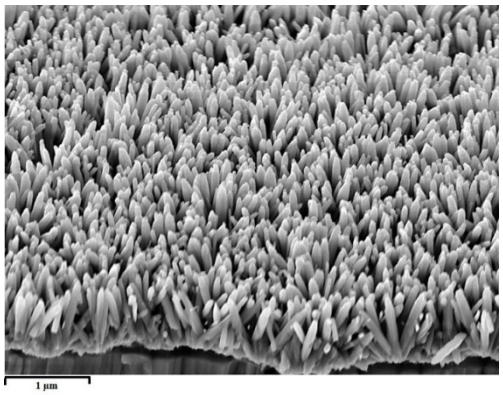

Fig. 5 ZnO nanorods grown on the top surface of ZnO thin film SAW device

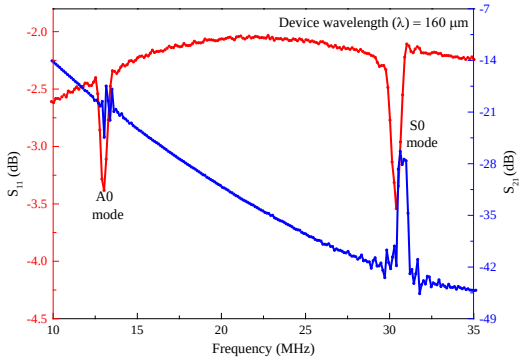

Fig. 6 Frequency response of the SAW device

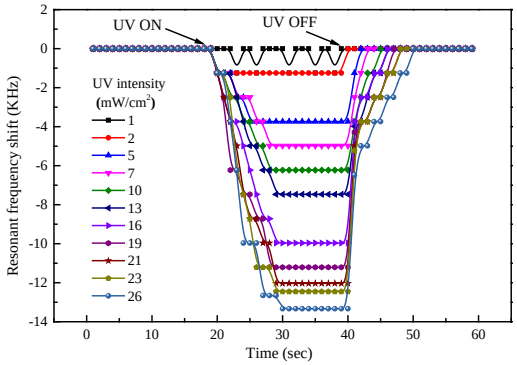

Fig. 7 Changes in resonant frequency of the A0 mode with UV light exposure when the device was kept flat. Reflection spectra were considered for the determination of the resonant frequency.

Figure 7 shows the changes in resonant frequency of the device under irradiation of UV light. Resonant frequencies of A0 mode at various UV intensities were firstly recorded when the device was kept flat. Reflection spectra were considered for the determination of the resonant frequency. The resonant frequency was shifted downwards when the device was exposed to UV light and the frequency shifts were increased with increasing UV light intensities. This mainly attributes to the increase of surface sheet conductivity (σ_s) due to the generation of electron-hole pairs of ZnO thin film when it is illuminated by UV photons. The temperature influence on frequency shift was not very significant as the temperature changes due to UV light was within ~1.2 ^{0}C. Thus, the increase of ZnO thin film conductivity (σ_s) causes a decrease of acoustic wave phase velocity according to equation 3, which is correlated with the resonant frequency by $f_o = v_0/\lambda$. The maximum shift obtained for A0 mode at flat position was 13 kHz.

The response time of the sensor after switching the UV light ON until reaches the maximum frequency shift was 10-12 seconds. The frequency shift is quite stable at this value as the photon generated carriers start to be saturated and thus there was no further change in the surface sheet conductivity of the thin film. However, the resonant frequency was shifted upward immediately once the UV light was switched OFF and it immediately reaches to ~60% of the maximum frequency shift. Then, depending on the UV light intensity used, it took 1-10 seconds to be completely recovered. This phenomenon is likely resulted from film defects that influence electron-holes recombination and oxygen adsorption.

The frequency shifts for both modes at different positions and various UV intensities can be seen in figure 8. It shows that the relationship between resonant frequency shifts and the UV light intensity is linear. This is due to the linear correlation between the concentration of the generated electron-hole pairs and the light intensity.

The slopes of these curves represent the rate of change in resonant frequency shifts over changes in UV light intensity ($\Delta f_0/\Delta I_{UV}$). The rate of change is decreased as the device is bent. This is likely due to the generated defects and the cracks during bending which influence the lattice structure of the thin film. Moreover, the rate is minimum when the device is bending up since more cracks and film defects are likely to occur. However, the internal stress of the film has no significant effect because the flexible bimorph structure of ZnO/Al-foil causes the film relaxation. The performance of the bent-down device is comparable to the flat one indicating that this bent-down device has much less cracks and defects. In addition, as the symmetric mode (S0) has a higher resonance frequency value, it shows larger changes of resonant frequency compared to the antisymmetric mode (A0).

The real time response of the flexible ZnO thin film based SAW UV sensor was further investigated to show the repeatability during UV light cycling as shown in figure 9. The sensor was illuminated with a UV intensity of 16 mW/cm^2 and the resonant frequency was decreased immediately when the UV light was switched ON. The response time holds almost the same value in all cycles (~10 seconds) and in each cycle the frequency shift reaches to a similar value or a saturation level.

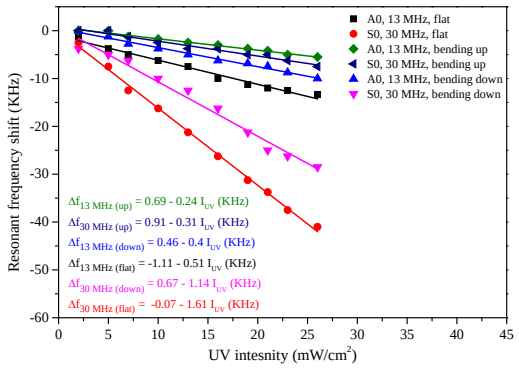

Fig. 8 Change in resonant frequency measured using S_{11} spectra for varying UV intensities for both zero order A0 and S0 modes

Moreover, as the UV light was switched OFF, the resonant frequency was increased and it reached the original baseline level within 8-10 seconds. The frequency response was stable and kept the same readings after five cycles that indicates excellent repeatability and stability of the sensor.

Figure 10 shows the change in resonant frequency measured using the S_{21} spectra for both vibration modes as a result of varied UV light intensities before and after growing the nanorods. The frequency shift has a nearly linear relationship with UV light intensity with and without nanorods. However, the change of frequency shift has been enhanced by 58% and 44% for A0 and S0 modes, respectively, when the nanorods were grown on the top surface of the device. This is mainly attributed to the fact that the nanorods have large surface to volume ratios that can enhance UV light absorption and increase the number of photo-generated carriers, and eventually influence the surface sheet conductivity and cause significant frequency shift.

The real time response of the nanostructured device exhibits very good repeatability and stability after five cycles as shown in figure 11. The resonant frequency does not reach a steady state or a saturation level and it was shifted slowly until it reaches to the maximum shift before the UV light was switched off. Similarly, it was shifted upward slowly toward the original baseline during the recovery stage. This indicates that the interaction between UV light and ZnO nanorods/ZnO film continued to generate more photo-carriers when the UV light was switched ON. In addition, it slows down the recombination process due to light scattering effect. This enhances the frequency shift and the sensitivity of the device.

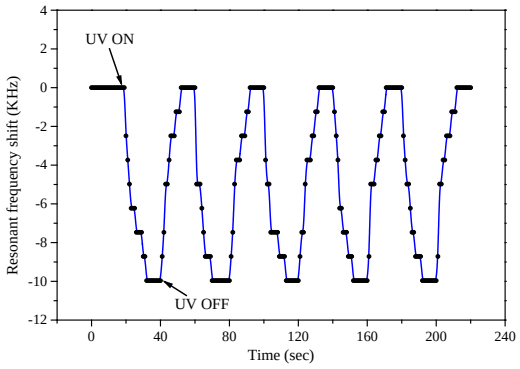

Fig. 9 Real time UV response (cycling) for A0 mode (13 MHz) using UV intensity of 16 mW/cm^2

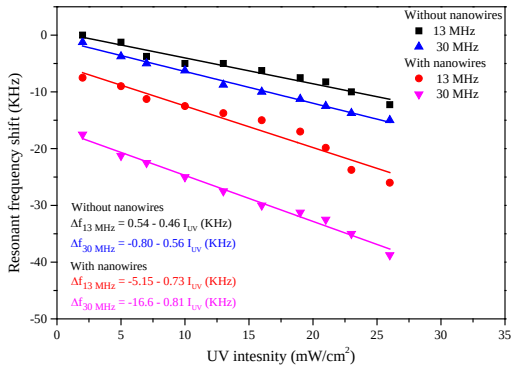

Fig. 10 Change in resonant frequency measured using S_{21} spectra for varying UV intensities with and without nanorods for both zero order modes

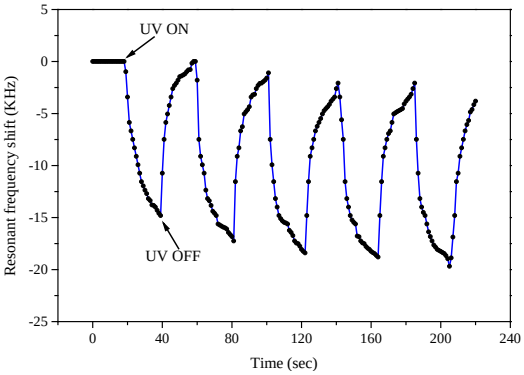

Fig. 11 Real time UV response (cycling) for A0 mode (13 MHz) with nanorods using UV intensity of 16 mW/cm^2

Table 1 summarizes the calculated sensor sensitivity for different modes, device positions and with nanorods enhancement. The UV light sensitivity of the SAW sensor is defined by the following formula [13]:

$$S_{UV} = \frac{1}{f_0}\frac{\Delta f}{\Delta I_{UV}} \qquad (4)$$

Where S_{UV} is the sensitivity, f_0 is the resonant frequency, Δf is the frequency shift, and ΔI_{UV} is the UV light variations.

The highest sensitivity for this Lamb wave sensor was 65.6 ppm (mW/cm^2)$^{-1}$ corresponding to A0 mode enhanced with nanorods. The sensitivity of S0 mode (without nanorods) at flat position was 53.7 ppm (mW/cm^2)$^{-1}$ which is comparable to the reported result in [13, 21].

Table 1 Device sensitivity for different modes, positions and with and without nanowires

Mode	**Resonant frequency (MHz)**	**S-parameter**	**Sample position**	**Sensitivity ppm(mW/cm^2)$^{-1}$**
A0	13	S11	Flat	37.7
S0	30	S11	Flat	53.7
A0	13	S11	Bending down	27.9
S0	30	S11	Bending down	37.9
A0	13	S11	Bending up	17.3

S0	30	S11	Bending up	10.3
A0	13	S21	Flat	35
S0	30	S21	Flat	18.7
A0	13	S21	Flat	65.6 (with NR)
S0	30	S21	Flat	27 (with NR)

The sensitivity values of the devices in the bending positions are between 10.3 and 37.9 ppm $(mW/cm^2)^{-1}$ where the minimum value was obtained when the device was bent up. However, the overall performance of this flexible ZnO thin film/Al-foil was promising and it has great potential to develop low cost flexible UV sensor for various applications.

IV. Conclusion

Flexible ZnO thin film based SAW device with a wavelength of 160 µm was successfully fabricated on a low cost commercial aluminium foil and it was used for UV light sensing. ZnO nanorods were further grown between the delay line region to enhance device's sensitivity. The film and the nanorods were characterized using SEM and XRD where the results showed good properties for piezoelectric functions. Two modes of vibration were identified; A0 and S0 and they were used to study the frequency response to UV light. The sensing performance of the sensor was investigated at different flexible positions: e.g., flat, bending down and bending up. The highest sensitivity obtained was 65.6 ppm $(mW/cm^2)^{-1}$ for nanorods enhanced device and 53.7 ppm $(mW/cm^2)^{-1}$ for non-enhanced one. The devices exhibited good repeatability and stability during real time measurements that indicates a great potential for these devices in applications as flexible or wearable UV light sensors.

References

[1] Y. Q. Fu, J. K. Luo, N. T. Nguyen, A. J. Walton, A. J. Flewitt, X. T. Zu, *et al.*, "Advances in piezoelectric thin films for acoustic biosensors, acoustofluidics and lab-on-chip applications," *Progress in Materials Science*, vol. 89, pp. 31-91, 2017/08/01/ 2017.

[2] B. Liu, X. Chen, H. Cai, M. Mohammad Ali, X. Tian, L. Tao, *et al.*, "Surface acoustic wave devices for sensor applications," *Journal of Semiconductors*, vol. 37, p. 021001, 2016.

[3] X. Ye, L. Fang, B. Liang, Q. Wang, X. Wang, L. He, *et al.*, "Studies of a high-sensitive surface acoustic wave sensor for passive wireless blood pressure measurement," *Sensors and Actuators A: Physical*, vol. 169, pp. 74-82, 2011/09/10/ 2011.

[4] X. Qiu, J. Zhu, J. Oiler, C. Yu, Z. Wang, and H. Yu, "Film bulk acoustic-wave resonator based ultraviolet sensor," *Applied Physics Letters*, vol. 94, p. 151917, 2009/04/13 2009.

[5] C.-L. Wei, Y.-C. Chen, C.-C. Cheng, K.-S. Kao, D.-L. Cheng, and P.-S. Cheng, "Highly sensitive ultraviolet detector using a ZnO/Si layered SAW oscillator," *Thin Solid Films*, vol. 518, pp. 3059-3062, 2010/03/31/ 2010.

[6] H.-F. Pang, Y.-Q. Fu, Z.-J. Li, Y. Li, J.-Y. Ma, F. Placido, *et al.*, "Love mode surface acoustic wave ultraviolet sensor using ZnO films deposited on 36° Y-cut LiTaO3," *Sensors and Actuators A: Physical*, vol. 193, pp. 87-94, 2013/04/15/ 2013.

[7] S. Y. Wang, Z. J. Li, X. S. Zhou, C. Zhao, X. T. Zu, and Y. Q. Fu, "Advances in Nanostructured Acoustic Wave Technologies for Ultraviolet Sensing," *Nanoscience and Nanotechnology Letters*, vol. 7, pp. 169-192, // 2015.

[8] A. J. Gimenez, J. M. Yáñez-Limón, and J. M. Seminario, "ZnO−Paper Based Photoconductive UV Sensor," *The Journal of Physical Chemistry C*, vol. 115, pp. 282-287, 2011/01/13 2011.

[9] X. Bian, H. Jin, X. Wang, S. Dong, G. Chen, J. K. Luo, *et al.*, "UV sensing using film bulk acoustic resonators based on Au/n-ZnO/piezoelectric-ZnO/Al structure," *Scientific reports*, vol. 5, pp. 9123-9123, 2015.

[10] A. J. Ricco, S. J. Martin, and T. E. Zipperian, "Surface acoustic wave gas sensor based on film conductivity changes," *Sensors and Actuators*, vol. 8, pp. 319-333, 1985/12/01/ 1985.

[11] W. Water, R.-Y. Jhao, L.-W. Ji, T.-H. Fang, and S.-E. Chen, "Love wave ultraviolet photodetector using ZnO nanorods synthesized on 90°-rotated ST-cut (42° 45′) quartz," *Sensors and Actuators A: Physical*, vol. 161, pp. 6-11, 2010/06/01/ 2010.

[12] S. P. Ghosh, K. C. Das, N. Tripathy, G. Bose, D. H. Kim, T. I. Lee, *et al.*, "Ultraviolet photodetection characteristics of Zinc oxide thin films and nanostructures," *IOP Conference Series: Materials Science and Engineering*, vol. 115, p. 012035, 2016.

[13] Y. J. Guo, C. Zhao, X. S. Zhou, Y. Li, X. T. Zu, D. Gibson, *et al.*, "Ultraviolet sensing based on nanostructured ZnO/Si surface acoustic wave devices," *Smart Materials and Structures*, vol. 24, p. 125015, 2015.

[14] T. Saha, N. Q. Guo, and N. Ramakrishnan, "Zinc Oxide Nanostructure-Based Langasite Crystal Microbalance Ultraviolet Sensor," *IEEE Sensors Journal*, vol. 16, pp. 2964-2970, 2016.

[15] V. Chivukula, D. Ciplys, M. Shur, and P. Dutta, "ZnO nanoparticle surface acoustic wave UV sensor," *Applied Physics Letters*, vol. 96, p. 233512, 2010/06/07 2010.

[16] J. Luo, X. He, J. Zhou, W. Wang, W. Xuan, J. Chen, *et al.*, "Flexible and Transparent Surface Acoustic Wave Microsensors and Microfluidics," *Procedia Engineering*, vol. 120, pp. 717-720, 2015/01/01/ 2015.

[17] J. Chen, X. He, W. Wang, W. Xuan, J. Zhou, X. Wang, *et al.*, "Bendable transparent ZnO thin film surface acoustic wave strain sensors on ultra-thin flexible glass substrates," *Journal of Materials Chemistry C*, vol. 2, pp. 9109-9114, 2014.

[18] Y. Liu, Y. Li, A. M. el-Hady, C. Zhao, J. F. Du, Y. Liu, *et al.*, "Flexible and bendable acoustofluidics based on ZnO film coated aluminium foil," *Sensors and Actuators B: Chemical*, vol. 221, pp. 230-235, 2015/12/31/ 2015.

[19] H.-S. Hong, D.-T. Phan, and G.-S. Chung, "High-sensitivity humidity sensors with ZnO nanorods based two-port surface acoustic wave delay line," *Sensors and Actuators B: Chemical*, vol. 171-172, pp. 1283-1287, 2012/08/01/ 2012.

[20] R. Tao, S. A. Hasan, H. Z. Wang, J. Zhou, J. T. Luo, G. McHale, *et al.*, "Bimorph material/structure designs for high sensitivity flexible surface acoustic wave temperature sensors," *Scientific Reports*, vol. 8, p. 9052, 2018/06/13 2018.

[21] X. L. He, J. Zhou, W. B. Wang, W. P. Xuan, X. Yang, H. Jin, *et al.*, "High performance dual-wave mode flexible surface acoustic wave resonators for UV light sensing," *Journal of Micromechanics and Microengineering*, vol. 24, p. 055014, 2014.